Direct simulations of compressible wall-bounded turbulence

By J. C. Buell

Several direct numerical simulations of high-speed turbulent Couette flow have been performed with a new spectral code. Mach numbers up to three and a Reynolds number of 3000 were used. A new time-integration scheme was developed to handle Mach numbers above 1.5, which require greater accuracy and stability than lower Mach numbers. At low Mach number, the large streamwise eddies found by M. J. Lee in his incompressible Couette flow simulations were reproduced. At higher Mach numbers these structures still exist, but they become considerably less organized (although the disorganization may be a function of the spanwise box size). While the same types of vortical structures seen in the incompressible flow are observed at higher Mach numbers, a new structure involving the divergence of the velocity is also observed. This structure is generally associated with low shear areas next to the walls, but it has not been determined whether it is a cause or an effect of the low shear. A "nonphysical" simulation was performed to determine by what mechanism the Mach number affects the flow. It appears that pressure gradient (acoustic) effects are more important than variable viscosity effects in determining the wall shear, but the size of vortical structures is determined more by the local kinematic viscosity. Low-order mean statistics are provided to help quantify these effects.

1. Motivation and objectives

Direct numerical simulations of incompressible turbulence have proven to be invaluable in describing physical mechanisms and quantifying various statistics that are essentially impossible to measure experimentally. For compressible flows, experimental measurements become even more difficult. Skin friction coefficients have been measured in several experiments with adiabatic walls (early results are summarized in Liepmann & Roshko 1957). These show a monotonic decrease with Mach number, but the mechanism is still not understood. Since little is known theoretically, a study was initiated to quantify the effects of compressibility (Mach number) on turbulent boundary layers. Our immediate objective is to be able to describe differences from the incompressible case in the turbulent structures and mean statistics. A longer-term goal is to use this information to improve turbulence models for high Mach-number boundary layers.

Couette flow with isothermal walls was chosen since it is one of the simplest flows in the desired class. The lack of a mean streamwise pressure gradient plus isothermal walls implies that both horizontal directions can be assumed to be homogeneous and that the flow can reach a statistically steady state. Together, these features greatly simplify the calculations and analyses of the results. The scales used for

nondimensionalizing the problem are the channel half-width (b), half the velocity difference between the walls (U_w), average density (ρ_a), wall temperature (T_w), and the fluid viscosity evaluated at the wall temperature (μ_w). In nonconservative form, the continuity, momentum and energy equations are

$$\frac{\partial \rho}{\partial t} + \rho \frac{\partial u_j}{\partial x_j} + u_j \frac{\partial \rho}{\partial x_j} = 0, \tag{1}$$

$$\frac{\partial u_i}{\partial t} + u_j \frac{\partial u_i}{\partial x_j} + \frac{1}{\gamma M^2} \frac{\partial T}{\partial x_i} + \frac{T}{\gamma M^2 \rho} \frac{\partial \rho}{\partial x_i} - \frac{1}{\rho Re} \frac{\partial \tau_{ij}}{\partial x_j} = 0, \tag{2}$$

$$\frac{\partial T}{\partial t} + u_j \frac{\partial T}{\partial x_j} + (\gamma - 1) T \frac{\partial u_j}{\partial x_j} - \frac{\gamma(\gamma - 1) M_d^2}{Re} \frac{\tau_{ij}}{\rho} \frac{\partial u_i}{\partial x_j} + \frac{\gamma}{\rho \, Re \, Pr} \frac{\partial q_j}{\partial x_j} = 0, \tag{3}$$

where

$$\tau_{ij} = \mu \left(\frac{\partial u_i}{\partial x_j} + \frac{\partial u_j}{\partial x_i} - \frac{2}{3} \delta_{ij} \frac{\partial u_k}{\partial x_k} \right), \qquad q_j = -\mu \frac{\partial T}{\partial x_j}.$$

The ideal gas relation $\rho T = \gamma M^2 p$ was used and the Reynolds and Mach numbers are defined by $Re = \rho_a U_w b / \mu_w$ and $M^2 = U_w^2 / \gamma R T_w$. The Prandtl number $Pr = c_p \mu^* / k^*$ and c_p are assumed to be constant throughout the flow (an asterisk is used to distinguish dimensional quantities). Note that in the dissipation term of (3), M is replaced with M_d. A "physical" simulation is obtained when $M_d = M$, but setting $M_d \neq M$ allows us to investigate the relative importance of the pressure gradient term in (2) and the energy dissipation term in (3). The main effect of the latter is to produce mean viscosity and conductivity profiles across the layer. Thus the two most important effects of M are acoustic and variable-property effects.

2. Accomplishments

2.1. Numerical method

The numerical method was described in Buell (1990a). Here we present a brief review of the spatial approximation and a short analysis of the time integration scheme needed for higher Mach numbers.

A classical Galerkin method is implemented in all three spatial dimensions. Thus the expansion functions and "test" functions are identical and satisfy all of the boundary conditions. Since the streamwise and spanwise directions are homogeneous, Fourier methods can be easily used. The implementation is similar to the incompressible direct simulation codes at NASA-Ames in that time advancement is performed in wave space which allows the Galerkin integrals to be performed more accurately (*i.e.*, dealiasing is done in physical space). This is unlike nearly all compressible codes; these typically use collocation methods and do not have any dealiasing at all. The complexity of the compressible equations prevents full dealiasing here, but the use of 30 to 50% more collocation points than modes comes close to eliminating aliasing errors since the strongest nonlinearity is still quadratic.

Because of the small grid size near the wall, an implicit treatment is needed for both the acoustic and diffusive terms. A straightforward implementation of

a spectral method requires that all implicit terms be constant-coefficient linear. The acoustic and diffusive terms are decomposed into a constant-coefficient linear part and a residual. This decomposition is given by Buell (1990a). It amounts to rewriting equations of the form

$$\frac{du}{dt} = \lambda u$$

as

$$\frac{du}{dt} = \lambda_0 u + (\lambda - \lambda_0)u,$$

where λ represents an eigenvalue of a spatial operator that one wants to treat implicitly. Since λ varies in space, a constant numerical parameter λ_0 is introduced so that the first term on the RHS above may be treated implicitly while the second term is treated explicitly. The appropriate value of λ_0 is determined by the range of λ and the time-integration scheme. For large $|\lambda|$, there is a maximum range over which λ can vary and still maintain stability for a single λ_0. This range is about $\lambda_{max}/\lambda_{min} = 2.4$ for the three-substep scheme described in Spalart *et al.* (1990), which is good enough for simulations using Mach numbers up to about 1.5. Motivated by the desire to simulate higher Mach numbers, a new four-substep scheme was developed. The coefficients were optimized so that absolute stability was obtained for $\lambda_{max}/\lambda_{min}$ up to at least 4.5, as well as achieving full third-order accuracy (previous schemes were second order for the implicit part). The new scheme is also stiffly stable (Gear 1971) for higher $\lambda_{max}/\lambda_{min}$, so that it appears that the algorithm will be stable for any Mach number. Details of the derivation and analysis of this scheme are given in Buell (1990b). The problem is that the above decomposition yields an increasing inaccurate time integration when $\lambda_{max}/\lambda_{min} > 5$. A new time integration scheme is still needed for hypersonic Mach numbers that does not require the implicit operator to be constant-coefficient linear.

Several different tests were used to check out the code. The best one consists of using eigenfunctions from a linear stability analysis (Buell 1990a) to verify that the growth rate can be reproduced by the nonlinear code. Many different 2-D and 3-D cases have been tried, and the numerical and linear stability results are always within 0.01 to 1% of each other. Even at $M = 8$, where the time integration is expected to be inaccurate, the results are very close. However, when random numbers or any profile other than an eigenfunction is used as an initial condition, the conclusions are not as clear. After the transient, the numerical growth (or decay) rate is close to linear theory, but only if the rate is averaged in time. Instantaneously, the growth rate oscillates around the average and the oscillations die out very slowly, if at all. We believe this behavior is physical, but do not have an explanation for it as yet.

2.2. Results

Shown in Table I are the four cases for which results are presented here. The Reynolds number is 3000 in all cases. Nx, Ny, and Nz are the number of modes in the three directions, and Lx and Lz are the periodic lengths in the two horizontal directions. The $M = 0.2$ case is marginally resolved, but the statistics compare very well with the better-resolved simulations of Lee (1990). The fluid is assumed

TABLE I

Numerical and physical parameters

case	Nx	Ny	Nz	Lx	Lz	M	M_d
1	60	48	90	12	8	0.2	0.2
2	110	64	60	12	4	1.5	1.5
3	110	64	60	12	4	1.5	0.2
4	90	90	60	10.6	4	3.0	3.0

TABLE II

Statistical properties

case	$\frac{d\bar{u}}{dy}\Big\|_w$	K.E.	$\bar{\rho}_w$	$\bar{\rho}(y=0)$	$\bar{T}(y=0)$
1	11.05	0.0147	1.0058	0.9996	1.0060
2	9.66	0.0130	1.3220	0.9767	1.3399
3	9.50	0.0127	1.0157	0.9974	1.0048
4	9.60	0.0135	2.2298	0.9294	2.3425

to be air with $Pr = 0.7$, $\gamma = 1.4$ and $\mu = T^{.7}$. The wall quantities (subscript w) are averages over time, the homogeneous directions, and both walls. K. E. is the average kinetic energy density over all three directions and time. Even at $M = 3$, the difference between standard and Favre averaging is negligible. The $M = 3$ case is the only one that is linearly unstable (Buell 1990a). Since only a very narrow range of wavelengths around the most unstable wavelength of 2.649 are unstable, we decided to use a box length that is an integral multiple (4) of this length. This guarantees that the flow cannot relaminarize. The spanwise box lengths were chosen based on the incompressible Couette flow results of Lee (1990). He found that large streamwise eddies form that scale on the channel height. With our nondimensionalization, a pair of these would have a width of about four. Since these structures are so large, it is impractical to use box sizes large enough so that the correlations become zero, as is usually the practice in direct simulations. The question of what is the appropriate box size (based on a "preferred" spanwise wavelength) and how it varies with the Reynolds and Mach numbers remains open.

2.2.1. Instantaneous fields

Shown in Figure 1 are representative contour plots of the streamwise velocity u at the midplane $y = 0$ for the three physical cases ($M = 0.2$, 1.5, 3). In all three cases, we see large streamwise structures dominating the flow. At $M = 0.2$, the flow is extremely close to being incompressible and the structures compare very well with the corresponding ones in the incompressible Couette flow simulations of Lee (1990). They are also similar to the structures at late time in homogeneous shear flow simulations (Lee, private communication). This indicates that walls are

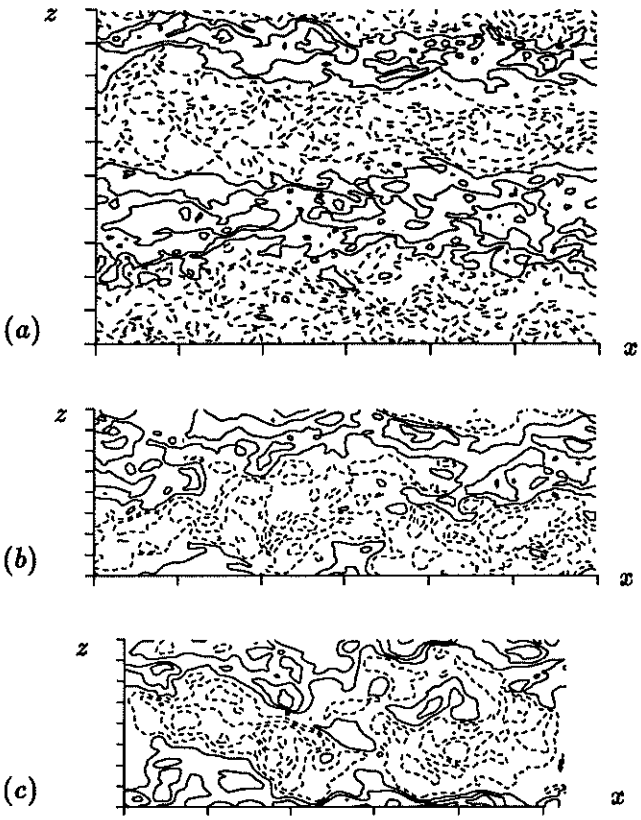

FIGURE 1. Streamwise velocity at $y = 0$ for (a) $M = 0.2$, (b) $M = 1.5$, and (c) $M = 3$. The contour interval is 0.1. Dashed lines denote negative values.

not necessary for their development. Higher Mach numbers appear to cause these structures to become less distinct. The dependence on Mach number appears to be related to boundary-layer effects, but it may be due to a change in the "preferred" spanwise wavelength. Also, the reduction in spanwise box size may allow the large structures to be less organized. This can be tested by performing a low M simulation with Lz = 4.

Figure 2 shows x–y cuts of ω_z through typical shear-layer structures for all four cases. We see that although the average shear at the wall is only about 13% smaller for $M = 3$ than for $M = 0.2$, the dominant vortical structures are about three times larger (extending up to $1 - |y| = 0.5$ instead of $1 - |y| = 0.15$ to 0.2). The vorticity magnitude in the shear layers and the peak values at the wall are correspondingly two to three times lower. Together with the qualitative appearance of the flow, this indicates that the global Reynolds number Re does not characterize the flow in the core of the channel. If the kinematic viscosity evaluated at the channel centerline is used instead of μ_w/ρ_a, then Re would be half as large for the $M = 3$ case as for the $M = 0.2$ case. This would be consistent with the appearances of the vortical structures, but not with the wall shear. Using wall variables to construct a Re_τ

does not provide a better overall scaling. Thus, it appears that there is no single definition of a Reynolds number that characterizes the entire flow. Data is given in Table II that can be used to construct other Reynolds numbers (the overbar represents a time and horizontal-space average).

We conjecture that the larger boundary-layer structures at $M = 3$ tend to break up the jet-like core flow. Increasing the Reynolds number so that the kinematic viscosity in the core matches that of the $M = 0.2$ case would verify this. A more precise comparison is given by the plots in Figure 2 and the data in Table II for the two $M = 1.5$ cases. The fact that the wall shear is independent of M_d indicates that the wall shear depends only on acoustic effects (M). However, the similarity of the vortical structures in the $M = 1.5$, $M_d = 0.2$ case to the $M = 0.2$ case indicates that these structures depend on the viscosity distribution, which is almost entirely dependent on M_d.

Shown in Figure 3 are organized structures of the divergence of velocity on the lower wall for the $M = 3$ case. These take the form of streamwise waves. x–y cuts (not plotted) show that the vertical extent is much smaller than the horizontal dimensions of each structure. Typically, they extend up to about $1 - |y| = 0.1$ with the core of the channel being nearly incompressible. Also shown are areas of low wall shear. The very good correlation with the divergence indicates that the two are related. It may be possible that the "divergence structures" cause the low shear; this would help explain the dependence of wall shear on M. On the other hand, they may be more passive, *i.e.*, a mode that is unstable under certain conditions but does little to affect the rest of the flow. Further investigation is needed to determine the cause and effect.

2.2.2. Statistics

The large length scales in turbulent Couette flow lead to large time scales and increased difficulty in obtaining converged statistics. The time scales are evident in Figure 4, where the average (in x and z) shear on both walls is plotted over the time interval in which statistics are gathered. Although the longest time scales are not well resolved, 300–500 time units is enough for the low-order statistics to be reliable. In particular, this is long enough for the total shear to be constant to within 2% across the channel.

Shown in Figure 5 are the mean profiles for u, ρ and T for the $M = 3$ case. Note that $\bar{\rho}$ and $\bar{T}$ are scaled with $K = \frac{1}{2}PrM^2(\gamma - 1) = 1.26$. This makes the profiles nearly independent of M (except near the walls, where the $M = 0.2$ case has slopes about 15% greater). This is especially true for temperature in the core: $(\bar{T}(y=0)-1)/K = 1.0660$ and 1.0656 for the $M = 0.2$ and $M = 3$ cases, respectively (the difference is not statistically significant).

The variance of each of the velocity components is shown in Figure 6 for the $M = 0.2$ and $M = 3$ cases. As was noted for the integrated kinetic energy, standard and Favre averaging yield the same results, at least up to $M = 3$. The $M = 0.2$ profiles are very close to the incompressible results of Lee (1990). In wall variables, the peak in the streamwise component is $u^+_{\rm rms} = 2.7$ and it occurs at $y^+ = 12$. There are two important differences between the two cases. First, the drop in the streamwise

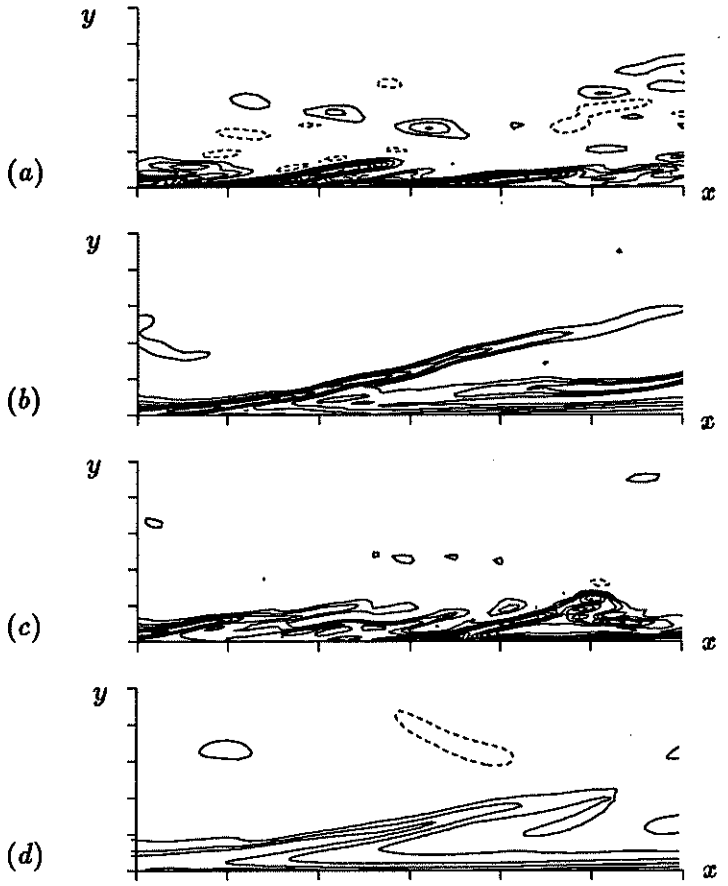

FIGURE 2. Spanwise vorticity $(-\omega_z)$ through typical shear layer structures for (a) $M = 0.2$, (b) $M = 1.5$, $M_d = 1.5$, (c) $M = 1.5$, $M_d = 0.2$, and (d) $M = 3$. The bottom half of the channel $-1 \leq y \leq 0$ and three units along the x-axis is shown in each case. The contour interval is 2.

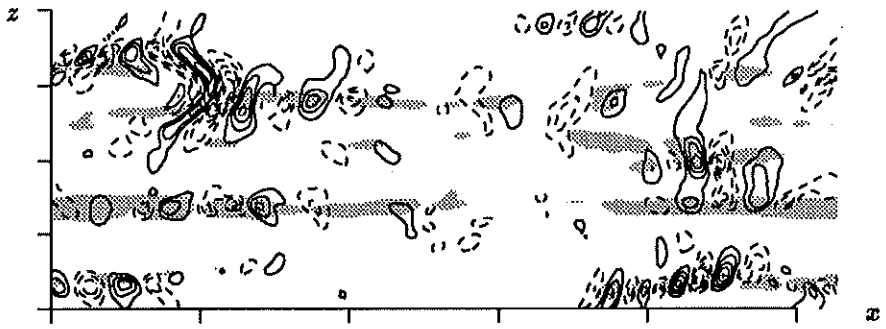

FIGURE 3. Divergence of the velocity at the lower wall for the $M = 3$ case. Contour interval is 0.2. Shaded areas denote low wall shear: $\frac{\partial u}{\partial y} < 5$.

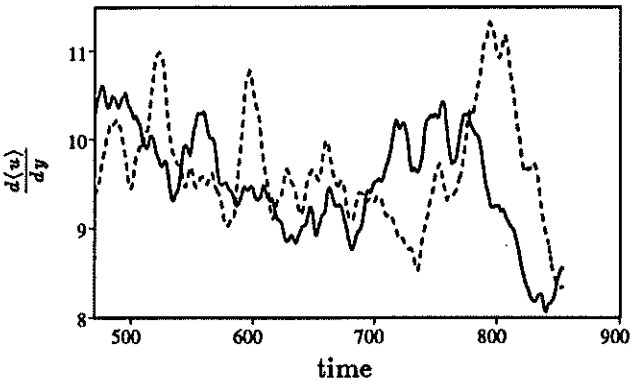

FIGURE 4. Horizontal average of $\frac{\partial u}{\partial y}$ on the lower wall (solid line) and upper wall (dashed line) for $M = 3$.

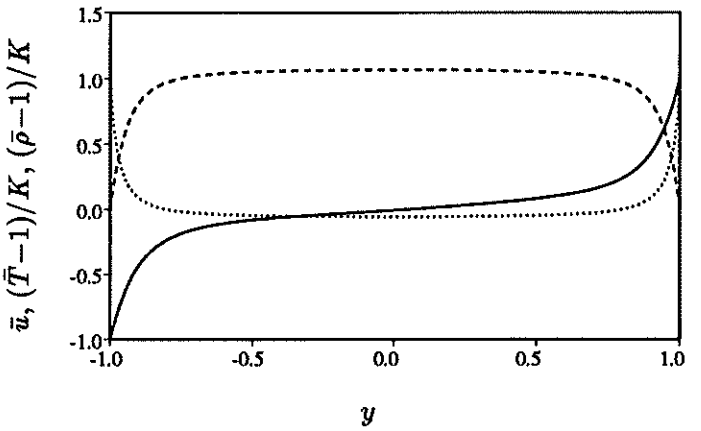

FIGURE 5. Mean profiles for u (solid), T (dashes) and ρ (dots) for $M = 3$. $K = \frac{1}{2}PrM^2(\gamma - 1)$.

component from its peak to its value at the channel center is much greater at the higher Mach number, while the other two components are qualitatively unchanged. This increased isotropy is apparently related to the break-up of the streamwise jets in the core. Second, the peak in the intensity occurs at $1 - |y| = 0.162$ for $M = 3$, but at $1 - |y| = 0.072$ for low Mach numbers. Unlike the relatively small differences in the absolute levels of the turbulence intensities, this difference cannot be scaled by any reasonable choice of the kinematic viscosity and velocity scale.

3. Future plans

We have presented here some results for compressible turbulent flow in a channel, but much work remains to be done in order to achieve our objectives. First, a higher Reynolds number $M = 3$ simulation should be performed where the kinematic

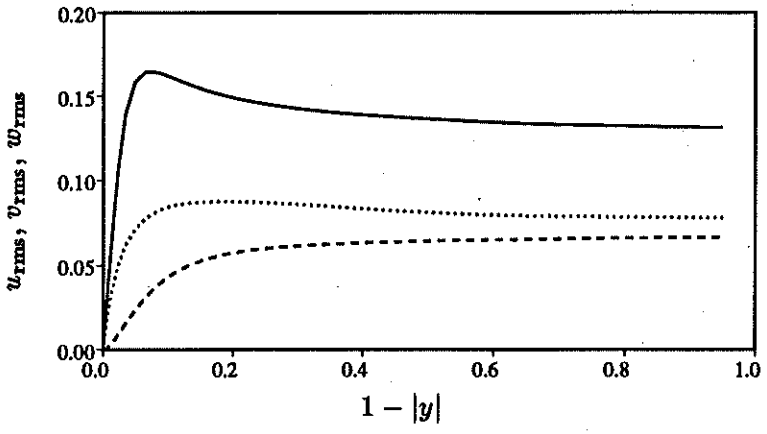

(a)

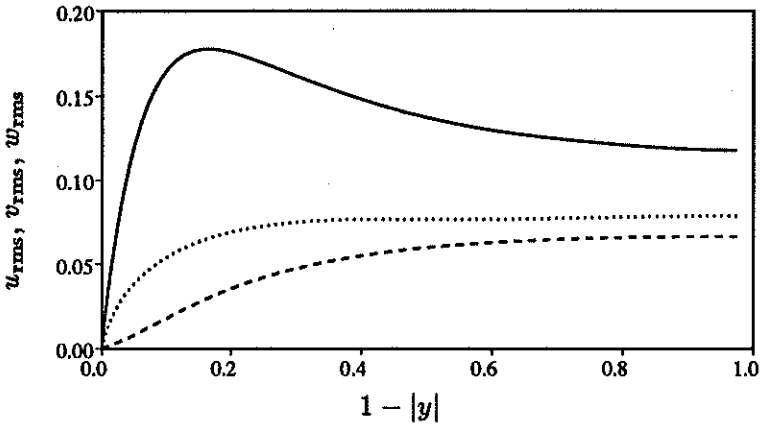

(b)

FIGURE 6. Profiles of the turbulence intensities for u (solid), v (dashes) and w (dots) for (a) $M = 0.2$, and (b) $M = 3$.

viscosity in the core matches that of the low Mach number simulations. This should be straightforward since the $M = 3$ simulation presented here was over-resolved, and since the temperature and density in the core appear to be easily predicted. Next, more realistic adiabatic or mixed boundary conditions need to be implemented for the temperature equation. This increases the implicit-operator bandwidth since the appropriate basis functions require three Legendre polynomials instead of just two. The computational cost of this will be minimal since linear algebra accounts for only about 10% of the run time now. Finally and most importantly, the simulation of higher Mach-number flows requires a different time integration scheme. The best way to do this is to generalize the decomposition (4) so that λ_0 is a low-order polynomial instead of just a constant. This will very effectively reduce the

magnitude of $(\lambda - \lambda_0)/\lambda_0$ and thus increase both the accuracy and stability of the time-integration scheme. The cost will be an increase in the matrix bandwidth by an amount proportional to the order of this polynomial. Fortunately, it appears that all of the x and z derivative operators may be treated explicitly, so that this matrix needs to be inverted only once per substep, at most.

REFERENCES

BUELL, J. C. 1990a Direct simulations of wall-bounded compressible turbulence. in *Annual Research Briefs - 1989.* Center for Turbulence Research.

BUELL, J. C. 1990b Third-order low-storage A-stable time integration schemes. submitted to *J. Comp. Phys.*

GEAR, C. W. 1971 *Numerical Initial Value Problems in Ordinary Differential Equations.* Prentice Hall.

LEE, M. J. 1990 The large-scale structures in turbulent plane Couette flow. in *Annual Research Briefs - 1989.* Center for Turbulence Research.

LIEPMANN, H. W. & ROSHKO, A. 1957 *Elements of Gasdynamics.* J. Wiley & Sons.

SPALART, P. R., MOSER, R. D. & ROGERS, M. R. 1990 Spectral methods for the Navier-Stokes equations with one infinite and two periodic directions. submitted to *J. Comput. Phys.*